Published in final edited form as:
Dev Dyn. 2013 October ; 242(10): 1184–1201. doi:10.1002/dvdy.24015.

Complex cardiac defects after ethanol exposure during discrete cardiogenic events in zebrafish: Prevention with folic acid

Swapnalee Sarmah and **James A. Marrs***
Department of Biology, Indiana University-Purdue University Indianapolis, Indianapolis, IN 46202

Abstract

BACKGROUND—Fetal alcohol spectrum disorder (FASD) describes a range of birth defects including various congenital heart defects (CHDs). Mechanisms of FASD-associated CHDs are not understood. Whether alcohol interferes with a single critical event or with multiple events in heart formation is not known.

RESULTS—Our zebrafish embryo experiments showed that ethanol interrupts different cardiac regulatory networks and perturbed multiple steps of cardiogenesis (specification, myocardial migration, looping, chamber morphogenesis and endocardial cushion formation). Ethanol exposure during gastrulation until cardiac specification or during myocardial midline migration did not produce severe or persistent heart development defects. However, exposure comprising gastrulation until myocardial precursor midline fusion or during heart patterning stages produced aberrant heart looping and defective endocardial cushions. Continuous exposure during entire cardiogenesis produced complex cardiac defects leading to severely defective myocardium, endocardium, and endocardial cushions. Supplementation of retinoic acid with ethanol partially rescued early heart developmental defects, but the endocardial cushions did not form correctly. In contrast, supplementation of folic acid rescued normal heart development, including the endocardial cushions.

CONCLUSIONS—Our results indicate that ethanol exposure interrupted divergent cardiac morphogenesis events causing heart defects. Folic acid supplementation was effective in preventing a wide spectrum of ethanol-induced heart developmental defects.

INTRODUCTION

Fetal Alcohol Spectrum Disorder (FASD), as a clinical entity, is associated with maternal alcohol consumption, producing a specific birth defect spectrum. Prenatal ethanol exposure causes central nervous system, craniofacial and body growth defects, and disrupts various organogenesis pathways, including heart. Babies born with FASD display various congenital heart defects (CHDs), which includes ventricular and/or atrial septal defects and conotruncal defects. It is unknown how alcohol consumption produces a wide spectrum of CHDs. This may be due to differences in timing (cardiogenic stage-dependent and/or duration dependent) and doses of alcohol exposure during heart morphogenesis. Among all FASD related CHDs, septal defects are the most frequently diagnosed anomalies (Burd et al.,

Author for correspondence: James A. Marrs, Department of Biology, Indiana University Purdue University Indianapolis, 723 West Michigan, Indianapolis, IN 46202-5130, Phone: 317-278-0031, Fax: 317-274-2846, jmarrs@iupui.edu.

2007). Ethanol exposures produce cardiac defects in animal models that are similar to human patients. In chick, acute ethanol administration at HH stage 18 (cardiac septation period) resulted in cardiac malformations, including ventricular septal defect (VSD) and overriding aorta (Fang et al., 1987). Alcohol induced VSDs occurred in chick embryos in a strain dependent way (Bruyere and Stith, 1993). In mice, Sulik and co-workers reported that acute ethanol exposure on gestational day (GD) 8 produced abnormal heart and defective great vessel formation (Daft et al., 1986). Alcohol exposure on GD 8, 9, 10 (somitogenesis period) in mice produced high incidence of VSDs, but exposure on day 7 (gastrulation) was resistant to the induction of heart defects (Webster et al., 1984). Recently, Linask and co-workers used echocardiography to identify embryos with heart valve regurgitation and reported that intraperitoneal injection (like a binge-drinking dose) of ethanol in mice on embryonic day 6.75 (gastrulation) produced atrioventricular and semilunar valve defects. In another study, Cavieres and Smith failed to reproduce valvoseptal defects in three chicken strains after ethanol exposure either during gastrulation, somitogenesis, or cardiac septation period (Cavieres and Smith, 2000). Additional model organisms that reliably reproduce defects to study FASD-associated heart defects are required.

Externally fertilized, transparent zebrafish embryos expressing fluorescent protein in the developing myocardium or endocardium would be instrumental for the analyses of ethanol effects in live embryos. Recent identification of the second heart field (SHF) supports the premise that zebrafish is a suitable system to model human CHDs (Lazic and Scott, 2011; Zhou et al., 2011a). Zebrafish embryos exposed to ethanol exhibited short body, craniofacial defect and microphthalmia, the characteristic features of FASD (Blader and Strahle, 1998; Kashyap et al., 2011, Marrs et al., 2010). Based on histology and heart rate analyses, Dlugos and Rabin demonstrated that continuous ethanol exposure during zebrafish embryogenesis altered heart morphology and function (Dlugos and Rabin, 2010). In zebrafish, heart morphogenesis begins at 5 hours post fertilization (hpf) when cardiac progenitors form in ventral and lateral regions of the embryo. Cardiac precursors reach anterior lateral plate mesoderm (ALPM) at around 5-somite (5s) stage (~12 hpf) and start to express cardiac specific genes. At 20s stage (~19 hpf), myocardial precursors fuse and form the heart cone. The heart tube is formed at 24 hpf. Heart primordia complete rightward looping at 36 hpf, and two distinct chambers arise. Finally, endocardial cells at the chamber boundaries undergo an epithelial-to-mesenchymal transition and form cardiac cushions, occurring around 48 hpf, eventually producing heart valves (Stainier, 2001). These critical cardiogenesis events are highly evolutionarily conserved within vertebrates. Subtle perturbation of these processes can cause severe physiological defects. Acute ethanol exposure during individual heart development stages and immediate analysis of cardiogenic events will help us understand alcohol effects on individual developmental events. Analyzing later stages will determine whether heart defects persist.

Various proposed mechanisms fail to completely explain the teratogenic effects of ethanol. Epidemiological studies showed that FASD incidence is higher in infants born to lower socioeconomic status alcoholic mothers compared to infants born to middle class alcoholics (Abel, 1995; Abel and Hannigan, 1995; Bingol et al., 1987). Lower socioeconomic population is at a greater risk for poor nutrition. Alcohol consumption also aggravates malnutrition by interfering with a person’s ability to absorb and use the nutrients they

consume, making the nutrient pool less than optimal for supporting fetal growth in alcoholic mothers (Abel and Hannigan, 1995). Alcoholics tend to have deficiencies in certain vitamins, including vitamin A and folic acid (FA) (Lieber, 2003). Vitamin A can be metabolized to retinoic acid (RA), which is essential for normal development, including heart. RA signaling plays multiple roles during cardiogenesis, including cardiac specification, anterior-posterior patterning, left-right specification, defining the limit of the second heart field, endocardial cushion formation and heart chamber growth (Hochgreb et al., 2003; Keegan et al., 2005; Ryckebusch et al., 2008; Sirbu et al., 2008; Waxman et al., 2008; Xavier-Neto et al., 2001). Many investigators hypothesized that abnormalities observed in FASD are caused by competitive inhibition of alcohol dehydrogenase catalyzed retinol oxidation by ethanol in the embryo, decreasing RA levels and signaling (Duester, 1991; Marrs et al., 2010; Yelin et al., 2005). Yelin et al. showed that ethanol exposure reduced the expression of *hox* genes in the *Xenopus* embryos, which are targets of RA signaling. Ethanol treatment rescued the effects of exposure to high levels of vitamin A (Yelin et al., 2005). Sulik and colleagues showed that ethanol treatment suppressed the expression of early limb genes in mice that could be phenocopied using an inhibitor that specifically blocks retinoid X receptor transcription factors (RXR, RA receptors) (Johnson et al., 2007). Another vitamin, folic acid, is essential for the synthesis, repair and regulation of DNA. FA is particularly important during rapid growth of the developing embryo. Studies showed that ethanol directly inhibits folate metabolism in cells and folate transport into cells (Ballard et al., 2012; Hamid and Kaur, 2007). A recent study demonstrated that FA transport to the fetus was impaired in pregnancies with chronic alcohol exposure (Hutson et al., 2012). Alcohol ingestion by animals inhibits folate-dependent DNA methylation (Ballard et al., 2012). Using mouse and avian models, Linask and co-workers showed that FA supplementation prevented ethanol-induced heart defects (Serrano et al., 2010). Epidemiologic studies showed that severe congenital heart defect prevalence was significantly reduced by prenatal FA fortification (Bailey and Berry, 2005; Ionescu-Ittu et al., 2009). These findings suggests that supplementation of essential nutrients may reduce the risk of CHD associated with FASD.

Aims of the present study were to examine the utility of the zebrafish as a model system to study FASD-associated CHDs, examine the ethanol effect on distinct cardiogenic events to determine whether heart developmental stages were differentially sensitive to ethanol in producing persistent heart defects. The effects of dosage and duration of ethanol exposure on heart development were also tested. Additionally, RA and FA were tested for their ability to prevent ethanol-induced cardiac defects in zebrafish.

RESULTS

Ethanol effects were analyzed using various assays, including live imaging of transgenic zebrafish lines *Tg[cmlc2:GFP]*, expressing GFP in myocardial cells, and *Tg[fli1:EGFP]*, expressing GFP in endothelial and endocardial cells.

Chronic ethanol exposure during embryogenesis severely disrupts heart morphogenesis

To model chronic ethanol exposure, embryos were exposed to ethanol from 2 to 48 hpf (Fig. 1A). Development of the heart was analyzed at 48, 52, 72 and 96 hpf. Ethanol exposed embryos displayed pericardial edema (Fig. 1B), aberrantly looped/straight heart at 48 hpf, which was worse at 72 hpf (Fig. 1 C, K). A small fraction of embryos also exhibited cardia bifida (Figs. 1K and 2D). These embryos never recovered, displaying severe cardiac defects including pericardial blood clot at 96 hpf (Fig. 1I, J). Examination of control *Tg[cmlc2:GFP]* embryos showed bean shaped atrium and ventricle closely apposed to each other with a narrow atrioventricular (AV) canal. Ethanol treated embryos showed smaller, misshapen myocardial chambers with a wider AV canal (Fig. 1D, Supp. Movies S1–S4). These embryos also displayed uneven ventricular wall and often had double lobed ventricle along the left/right axis, at higher frequency with 150 mM ethanol treatment (Fig. 1E, F, J, Supp. Movies S1–S4). To analyze ventricular defects in detail, cardiomyocyte numbers were counted at 52 hpf. Ethanol treatment reduced ventricular cardiomyocytes (VC) in a dose dependent way (control, VC=112±5; ethanol-100mM, VC=83±5; ethanol-150mM, VC=66±4 cells, $P< 0.008$). To understand ventricular wall defect cardiomyocyte morphology was assessed with alcam antibody staining, an adhesion protein expressed at embryonic myocardium cell-cell borders. Zebrafish ventricular cardiomyocytes dramatically change shape in a regionally confined manner during chamber growth, from 48–58 hpf (Auman et al., 2007). Distinct cardiomyocyte shape changes occur in the three major regions of the cardiac wall, outer curvature (OC), inner curvature (IC), and AV canal. Initially small, round cardiomyocytes in the heart tube undergo cell shape changes, producing large, elongated cardiomyocytes in the OC and AV region, but IC cardiomyocytes remain round and small (Auman et al., 2007). Control embryo heart showed these cell shapes (Mean surface area, OC=124±27 μm^2; IC=73±19.μm^2; Fig. 2B). Regional confinement of similar shaped cardiomyocyte was hard to distinguish and alignment of cells was highly disorganized after ethanol exposure (Fig. 2C). Although, 100mM ethanol treated embryos displayed elongated cells in the OC region (Mean surface area of elongated cells, 86±26 μm^2), circular cells were often found close to elongated cells. A few thin, elongated cardiomyocytes were present in the mid-region of the ventricular wall in ethanol exposed embryos with double lobed ventricles (Fig. 2C). Cell shape change was rare in 150 mM ethanol treated embryos (Mean surface area, 37 μm^2±30). Alcam staining also showed cardia bifida in ethanol treated embryos (Fig. 2D).

Examining live *Tg[fli1:EGFP]* embryos at 48 and 72hpf showed misshapen endocardium in ethanol treated individuals (Fig. 1G). Texas red-phalloidin stained (detecting F-actin) *Tg[fli1:EGFP]* embryos showed that endocardial lining corresponded to the shape of the myocardial layer (Fig. 1H). Endocardial cushions, precursor of heart valves, form at the AV canal by endocardial cells epithelial-to-mesenchymal transformation, where differentiated endocardial cells delaminate, invade and cellularize the extracellular matrix between myocradium and endocardium (Staudt and Stainier, 2012). Differentiated endocardial cells (cushion forming cells) express high levels of F-actin (Bartman et al., 2004; Beis et al., 2005). Endocardial cushion formation was analyzed in the *Tg[fli1:EGFP]* embryos at 52 hpf by Texas red-phalloidin staining. Control embryos showed a cluster of GFP and F-actin positive cuboidal shaped cells at the AV boundary, but ethanol treated embryos displayed

fewer or no clustered GFP and F-actin positive cells at the AV boundary (Fig. 2E–G). Together, these results indicate that ethanol exposure during all cardiogenesis stages severely disrupts myocardium, endocardium, and endocardial cushion morphogenesis. Higher concentrations of ethanol produce more severe phenotypes.

Ethanol exposure during cardiac specification perturbs cardiac gene expression, but heart defects do not persist

To determine whether ethanol exposure during initial stages of cardiogenesis, gastrulation until cardiac specification, produces heart defects at later stages, embryos were treated with ethanol from 2 hpf to 12s stage (Fig. 3A). Ethanol exposure caused a developmental delay. Control embryos reached 12s at 15 hpf; 100 mM ethanol treated embryos reached 12s at 15.5 hpf; and 150 mM ethanol treated embryos reached 12s around 15.75 hpf. Thus, somite numbers (hpf, corresponding developmental timing of control embryos) were used to match similar developmental stages instead of developmental time at early stages.

Expression patterns of myocardial induction gene *fgf8a* and cardiogenic transcription factors *nkx2.5* and *gata5* were examined at 13s (15.5 hpf) stage by in situ hybridization (ISH). ISH results showed moderate expansion of these expression domains in the ALPM region in ethanol treated embryos compared to controls (Fig. 3B–D). Quantitative PCR was used to examine early transcription factors required for heart formation at 6s (12 hpf) and 12s (15 hpf) stages. The expression of *gata5* and *hand2* showed significant upregulation after ethanol treatment at 12s (Fig. 3E). However, transcript levels of other cardiogenic genes tested did not show significant changes (Fig. 3E). Cardiac cone formation was analyzed at 20s stage (19 hpf) using cardiac myosin light chain (*cmlc2)* ISH. Myocardial cells in 20s control embryos migrated from the ALPM to the midline and fused to form the heart cone. In 100 mM ethanol exposed 20s embryos, only posterior fusion of myocardial cells was observed, and 150 mM ethanol treated 20s embryos exhibited two separate, unfused rows of myocardial precursors (Fig. 3F, I). Interestingly, these embryos showed relatively normal hearts at 36 and 60 hpf, with normal cardiac looping and heart chambers (Fig. 3G). Similar to myocardial cells, examination of *Tg[fli1:EGFP]*embryos at 19s stage showed delayed fusion of endocardial cells in the ethanol exposed embryos; those embryos exhibited near normal endocardium at 44 hpf (Sarmah and Marrs, unpublished observations).

To examine whether early ethanol exposure affects endocardial cushion formation, *bmp4* ISH was performed at 48 hpf. The expression of *bmp4* was prominent in the AV canal and outflow tract (OFT) in the control embryos. Ethanol exposed embryos exhibited *bmp4* expression pattern that was indistinguishable from control embryos (Fig. 3H). Taken together, these results show that ethanol exposure during cardiac specification expands cardiogenic gene expression domain in the embryo and delays myocardial cone formation. Embryos recover from this developmental delay and show no detectable, persistent cardiac defects.

Ethanol exposure until cardiac fusion stage produces persistent heart developmental defects

To determine whether ethanol exposure for a longer time period (gastrulation until myocardial midline fusion) produces persistent heart defects, embryos were ethanol treated from 2 hpf to 20s stage (Fig. 4A). ISH to detect *cmlc2* and *ventricle myosin heavy chain* (*vmhc)* expression revealed that ethanol exposure significantly delayed myocardial cone formation. By 19s (18.5 hpf) stage, myocardial precursors fused posteriorly in control embryos (99%, n=60), but myocardial precursors in 100 mM ethanol exposed embryos remained separated (97%, n=65) (Fig. 4B). The cone formation delay was more severe in 150 mM ethanol treated embryos, displaying two widely separated rows of myocardial precursors (100%, n=59) (Fig. 4B). Mantel-Haenszel chi-square tests revealed significant changes ($P<0.0001$) for both control vs. EtOH-100 and control vs. EtOH-150. Delayed posterior fusions of myocardial cells were visible until around 25s stage (Fig. 4C, D).

Similar to myocardial cells, bilateral endocardial precursors originate at ALPM, migrate to the midline and fuse. Ethanol exposed (2 hpf to 20s) *Tg[fli1:EGFP]* embryos showed delayed fusion of endocardial precursors at 20s stage (Fig. 4G). Endocardial lining (at 24 hpf; Fig. 4H) was abnormal, perhaps corresponding to the heart tube defect.

In utero alcohol exposure reportedly alters directional asymmetry in patients' faces (Klingenberg et al., 2010) and left-right dominance in the frontal brain lobe (Riikonen et al., 1999). To examine whether ethanol exposure (2 hpf to 20s) altered cardiac asymmetry or caused cardia bifida, *bmp4* expression was analyzed by ISH. At 20 hpf, *bmp4* was predominantly expressed on the left side of the heart field in the control embryos (Fig. 4E). Ethanol exposed 20 hpf embryos displayed an expression pattern similar to the *bmp4* expression in the younger embryos (14–19s; Thisse, 2005) (Fig. 4E′), showing a developmental delay. At around 25 hpf, when control embryos displayed *bmp4* expression in the linear heart tube, ethanol treated embryos exhibited asymmetric *bmp4* expression similar to the control embryos at 20 hpf (Fig. 4F–F‴). Higher *bmp4* expression on the left side of the ethanol exposed heart indicating delayed establishment of normal cardiac asymmetry.

To measure early ethanol exposure effects (2 hpf to 20s) on heart development, cardiac looping angles were measured in *Tg[cmlc2:GFP]*embryos at 36 hpf and 60 hpf. The "looping angle" was defined as the angle between the antero-posterior axis of the embryo and the plane of the atrioventricular junction (Chernyavskaya et al., 2012). Ethanol exposed embryos exhibited reduced looping, producing significantly greater average looping angle than control embryos (Fig. 4I, J).

Endocardial cushion formation was defective after early ethanol exposure. Unlike control embryos where *bmp4* expression was prominent in the AV boundary and OFT, ethanol exposed embryos displayed strong ectopic expression of *bmp4* throughout the ventricle at 48 hpf (Fig. 4K). Accordingly, *Tg[fli1:EGFP]* and F-actin positive cells, that were clustered at the AV boundary in the control embryos, were dispersed in the ventricle in the ethanol exposed embryos at 52 hpf (Fig. 4L, M).

These experiments raise two possibilities: (i) the observed cardiac defects were due to cumulative ethanol exposure during gastrulation through midline fusion (2 hpf–20s); or (ii) due to ethanol exposure only during the myocardial migration event (12s–20s). To investigate that possibility, embryos were treated with ethanol from 12s to 20s stage and *cmlc2* expression was examined at 20s stage (Fig. 4N). A slight delay in myocardial migration was detected between the control and ethanol treated embryos (Fig. 4O–R), indicating that more persistent, severe heart defects require ethanol exposure for a longer period.

Ethanol exposure during cardiac patterning caused heart morphogenesis and endocardial cushion defects

Effects of ethanol exposure during cardiac patterning (heart tube and loop formation) stages (20s until 36 hpf) was studied next (Fig. 5A). Ethanol exposure during cardiac patterning delayed cardiac looping, as revealed by *cmlc2* ISH (Fig. 5B, C) and live imaging of *Tg[cmlc2:GFP]* embryos. Although the degree of looping was reduced, all ethanol treated embryos displayed rightward looping around 40 hpf as seen in fixed *Tg[cmlc2:GFP]* embryos. Cardiac chambers were smaller and elongated, and AV canals were defective in these embryos (Fig. 5D). Texas red-phalloidin stained ethanol exposed *Tg[fli1:EGFP]* embryos confirmed defective endocardial cushions, exhibiting GFP and F-actin positive cells throughout the ventricle, without evident clustering at the AV boundary (Fig. 5E; compare control panels Figs. 2E and 4L).

To determine whether ethanol exposure prior to cardiomyocyte shape change affects regionally confined cell shape changes, embryos were alcam stained at 40 and 52 hpf. At 40 hpf, small, rounded cells were present throughout the ventricle wall in 150 mM ethanol exposed embryos, but elongated cells were apparent in the control and 100 mM ethanol treated embryos. At 52 hpf, ethanol exposed embryos exhibited surface area of OC cardiomyocytes similar to control OC cardiomyocytes [Mean surface area (OC): control, 118±35 μm^2; E-100mM, 108±30 μm^2; 107±23 μm^2; P value was not significant; Fig. 5F]. These findings indicate that ethanol exposure during cardiac patterning was detrimental, leading to heart valve and chamber morphology defects, however, regionally confined cardiomyocyte shape changes was not perturbed.

Ethanol exposure during chamber growth stage caused minor developmental perturbation

To determine whether ethanol affects cell shape changes during chamber morphogenesis (when zebrafish ventricular cardiomyocytes dramatically change shape) leads to ventricular wall defects, embryos were treated with ethanol from 40 to 56 hpf (Fig. 5G). Confocal imaging of *Tg[cmlc2:GFP]* embryos revealed slightly smaller but otherwise normal looking chambers in ethanol exposed embryos (Fig. 5H). Those embryos showed relatively normal cardiac looping angles (Fig. 5H). Alcam staining at 56 hpf showed few or no effects on cardiomyocyte shape changes comparing control and ethanol treated embryos (Fig. 5I). These findings show that ethanol exposure during cardiac growth had few effects on heart development.

RA supplement partially restores ethanol-induced early cardiac defects, but A-V canal defects remain

It was previously shown that 1 nM RA supplement could rescue a spectrum of ethanol-induced defects produced by 100 mM ethanol exposure in zebrafish without causing distinguishable RA induced defects (Marrs et al., 2010). Here, RA supplementation was tested for rescue of ethanol-induced cardiac defects. Co-supplementation of 1 nM RA with ethanol during cardiogenesis, from 2 to 48 hpf (Fig. 6A) rescued ethanol-induced small eye and body length defects (Fig. 6B–M). However, RA supplementation could not rescue heart edema (Fig. 6H–M). Although the chamber size was improved over ethanol treated embryos, RA plus ethanol treated embryos had either straight or reduced heart looping, and endocardial cushions were malformed (Fig. 6N–Y). However, unlike ethanol treated embryos (displaying fewer or no endocardial cushion cells), ethanol plus RA treated embryos showed endocardial cushion cells dispersed throughout the ventricle (Fig. 6T–Y). It was previously reported that 10 nM RA supplementation during HH stage ~8 (~26 hpf) to ~48 hpf rescued ethanol-induced heart looping defect in quail embryo culture (Twal, 1997). Next, RA supplementation during different cardiogenic events were tested, which would test a less stringent requirement for rescue in a shorter developmental period. Contrary to the prolonged treatment, co-supplementation of RA with ethanol during early cardiac specification (2 hpf to 12s) significantly restored *nkx2.5* expression and partially rescued myocardial migration delay (Fig. 7A–D). Myocardial migration delay was also partially rescued by co-treating embryos with RA and ethanol until myocardial fusion (2 hpf to 20s), as shown by *cmlc2* ISH at 20s stage (Fig. 7E–G). However, embryos co-treated with RA until 20s stage exhibited defects in endocardial cushion formation at 52 hpf. *Tg[fli1:EGFP]* embryos co-treated with ethanol and RA (2 hpf to 20s) displayed little or no clustering of GFP and F-actin positive cells at the AV boundary, which were instead dispersed throughout the ventricle (Fig. 7H). To determine whether RA supplementation could rescue cardiac defects caused by ethanol exposure during cardiac patterning, embryos were co-treated with ethanol and RA from 20s until 36 hpf (Fig. 7I). Examining cardiac looping in *Tg[cmlc2:GFP]* embryos at 36 hpf showed significant rescue after RA supplement (Fig. 7J, K). Interestingly, endocardial cushion cells showed a dispersed pattern in ethanol plus RA treated (20s until 36 hpf) *Tg[fli1:EGFP]* embryos at 52 hpf (Fig. 7L). These findings provide evidence that RA supplement could restore ethanol-induced defects of gene expression during specification, heart cone formation, and cardiac looping but not the endocardial cushion formation defect.

Folic acid supplementation prevents ethanol-induced heart defects more effectively than RA

FA supplementation was tested for rescue of ethanol-induced ethanol-induced cardiac defects in zebrafish. Co-treating zebrafish embryos with 50 μM FA and ethanol during entire cardiogenesis (2 to 48 hpf) partially rescued cardiac edema, but co-treatment with 75 μM FA (2 to 48 hpf) significantly rescued cardiac edema, small eye, and body length defects seen in embryos exposed to ethanol alone (Fig. 8A, B). Ethanol and FA co-treated *Tg[cmlc2:GFP]* and embryos showed normal heart tube at 24 hpf (Fig. 8C). At 52 hpf, ethanol and FA co-supplemented embryos exhibited near normal myocardium morphology (Fig. 8D; Supp.

Movies S1, S2 and S5). *Tg[fli1:EGFP]* embryos co-supplemented with ethanol and FA showed normal endocardium formation at 28 hpf and 52 hpf (Fig. 8E, F). GFP and F-actin positive endocardial cushion cells were rescued by co-treatment of FA with ethanol in Texas red-phalloidin stained *Tg[fli1:EGFP]* embryos (Fig. 9B–G). Alcam-stained FA and ethanol co-treated *Tg[cmlc2:GFP]* embryos showed region specific cardiomyocyte shape (Mean surface area, OC: E-100+FA, 117±27 μm^2; E-150+FA, 120±21 μm^2; IC: E-100+FA, 61±10 μm^2; E-150+FA, 62±14 μm^2), restoring ventricular wall morphology (Fig. 9H–M). Unlike RA, FA supplementation was able to significantly prevent cardiac defects in embryos, even when exposed to stringent, chronic ethanol exposure regimen (Fig. 9N). These findings showed that FA is a better supplement than RA that rescued a more complete spectrum of cardiac defects including endocardial cushion defect, in addition to other ethanol-induced defects.

DISCUSSION

Our experiments demonstrated that ethanol exposed zebrafish embryos exhibit cardiac defects including valve formation defects. This study differs from previous studies of animal models in various ways. First, we examined a chronic alcohol exposure model, exposing embryos during all cardiogenesis stages. Second, we analyzed ethanol effects on both myocardium and the previously unexplored endocardium development in live embryos. Third, we used acute ethanol exposure regimens to target different heart development stages: i) gastrulation through cardiac specification; ii) gastrulation through myocardiocyte midline fusion; iii) cardiac patterning; and iv) cardiac growth. For the above time periods, we systematically analyzed acute effects of ethanol exposure, and the persistence of these cellular and molecular effects in hearts at later larval stages. Our results support the idea that the wide varieties of FASD-associated CHDs reflect differences in ethanol dosage and exposure timing during heart development.

Ethanol exposure alters multiple steps of cardiogenesis

Ethanol interrupts multiple cardiogenesis events (specification, myocardial migration, looping, chamber morphogenesis and endocardial cushion formation). Perturbation of multiple/regulatory networks solely by ethanol epitomizes the complexity of FASD phenotypes and suggests that a single mechanism alone cannot explain the entire spectrum of ethanol-induced cardiac defects. Ethanol treatment did not randomize left-right heart asymmetry. Although critical cardiac development events were sensitive to ethanol, short exposure windows only during cardiac specification or only during myocardial migration did not produce severe or persistent heart development defects. Zebrafish embryos possess sufficient plasticity to recover from these developmental delays and produce a relatively normal embryo. An ethanol exposure window from gastrulation until myocardial migration caused heart defects including endocardial cushion defects that persist into later larval stages, suggesting that combined effects on these stages are responsible for the most severe phenotypes. Ethanol exposure during cardiac patterning stage (20s to 36 hpf) produced similar cardiac phenotypes as those produced by ethanol exposure from gastrulation until myocardial migration stages. How did ethanol exposure at different heart development stages produce similar heart phenotypes? Cardiac development requires multiple progenitor

cell types: first heart field, second heart field, and cardiac neural crest cells (Lin, C, 2012). These progenitors are derived in different locations in the embryo and are incorporated into the heart at different developmental stages. Ethanol exposure at different heart development stages might affect various progenitor cell types differentially. Future study is needed to better understand ethanol effect on different cardiac progenitors including their incorporation into the heart.

Chronic alcoholism and cardiac defects

Our study demonstrated that chronic ethanol exposure produced more complex phenotypes than ethanol exposure at a specific heart development stage. Chronic exposure produced straight heart that appeared smaller and very defective ventricle with double lobes. However, there was no internal tissue detected that separated the ventricular chamber as indicated by confocal optical sections of TO-PRO 3 stained *Tg[cmlc2:GFP]*embryos and actin stained Tg[fli1:EGFP] embryos.

Our study showed previously unappreciated effects of ethanol on ventricle chamber regionally confined cardiomyocyte shape changes. Smaller ventricle is because of reduced cardiomyocyte number and cardiomyocyte size. Endocardial cushion defects caused by chronic ethanol exposure (2–48 hpf) were more severe than defects seen after short ethanol exposure (2 hpf–20s or 20s–36 hpf). Chronic exposure almost completely eliminated endocardial cushion cells. In contrast, short exposures had a less severe phenotype, showing differentiated endocardial cells that are not at the AV boundary, but are instead dispersed throughout ventricle. Chronic alcohol consumption during pregnancy in humans may affect multiple steps of heart development, leading to complex cardiac defects (showing more than one congenital heart defect). Complex cardiac defects were common among offspring of chronic alcoholic mothers (Strandberg-Larsen et al., 2011).

Possible mechanisms of ethanol-induced cardiac defects

Numerous potential mechanisms were previously proposed to explain ethanol effects on the developing embryo, for example: 1) Changes in gene expression including retinoic acid signaling activity; 2) Increased oxidative stress-excess free radical and reduced antioxidant level; 3) Changes in cell adhesion; 4) Increased cellular apoptosis; and 5) Disrupted cellular metabolism (Abel, 1998; Mitchell et al., 1999). Our chronic vs. acute ethanol exposure analysis supports the idea that multiple mechanisms may act concurrently or consecutively, and thus, severity of ethanol-induced defects could vary due to developmental stage, dosage and duration. For example, ethanol exposure during cardiac looping (20s to 36 hpf) did not produce straight heart, but this treatment reduced the extent of cardiac looping. On the other hand, chronic exposure more completely blocked the looping process, producing straight heart. Similarly, ethanol exposure during the chamber cardiomyocyte shape change period (from 40–56 hpf) did not affect the regionally confined cell shape changes, but chronic exposure persistently affected this event. Together, these findings support a model that consecutive detrimental effects on multiple developmental events and mechanisms cause ethanol-induced heart defects.

During cardiogenesis, ethanol could affect various dynamic processes. Directional cell migration defects may participate in ethanol-induced cardiac specification and myocardial migration defects. Studies showed that ethanol interfered with convergence extension movements during early development (Yelin et al., 2005; Zhang et al., 2010). Reduced directional cardiac precursor migration probably expands the heart field region, resulting in their dispersion in a larger area of ALPM. Myocardial migration to the midline and subsequent rotation to form a linear tube was defective after ethanol exposure as observed in live *Tg[cmlc2:GFP]* embryos by time lapse imaging (SS and JAM, unpublished data). Developmental delay could also disrupt normal tissue interactions, causing ethanol-induced malformations. Interestingly, the rate of ethanol-induced developmental delay was not uniform throughout the embryo, but varied from organ to organ. Somite development was relatively faster than cardiac cone formation. Control embryos reached 20s at 19 hpf, but 100 mM ethanol treated embryos reached 20s almost half an hour later, at around 19.5 hpf. Cardiac cone was formed at 19 hpf (20s) in the control embryos. In 100 mM ethanol exposed embryos, cardiac cone started to form at around 23 hpf, at 25s stage. These developmental delays could produce asynchronous morphogenesis and tissue interaction events. For example, some ethanol treated embryos showed cardiomyocyte rotation prior to their proper fusion at the midline, leading to cardia bifida. Endocardial cushion formation was the most ethanol sensitive event detected in our study. Endocardial cushion originates from three different progenitor populations in mammals: endocardial; SHF; and cardiac neural crest cells (Lin et al., 2012). Our study demonstrated that ethanol exposure caused defective endocardium morphogenesis in zebrafish that could lead to the endocardial cushion defect. Ethanol exposure reduced the expression of *Islet 1,* a marker for SHF (Serrano et al., 2010). Future study is needed to examine potential effects of ethanol on different progenitor populations.

Retinoic acid and folic acid protection

Our study demonstrated that RA co-supplement for short durations was able to partially rescue ethanol-induced cardiac specification, migration, and looping defects. RA supplement during cardiac specification restored the *nkx2.5* expression pattern in the cardiac field. RA signaling from the developing somites restricts posterior boundary of the cardiac field during specification. Weak RA signaling presumably led to the expansion of *nkx2.5* expression antero-posteriorly, and thus, providing RA exogenously at this stage helped restore normal *nkx2.5* expression patterns. RA signaling is also necessary for cardiac looping. RA deficient *Raldh2*$^{-/-}$ knockout mouse embryos failed to undergo heart looping (Niederreither et al., 2001). Reduced RA might have caused reduced cardiac looping in the embryos exposed to ethanol, and exogenous RA supply from 20s–36hpf period helped restore normal cardiac looping. However, continuous exogenous supply of RA was not very effective in preventing chronic ethanol exposure associated heart defects, but RA was able to rescue some other ethanol-induced defects such as small eye and short body. Endocardial cushions defects caused by ethanol exposure could not be rescued by 1 nM RA supplement. It may be possible that treatment with different RA concentrations during endocardial cushion formation period would rescue this defect, but this has not been analyzed.

Maternal FA deficiency is associated with neural tube and congenital heart defects. FA supplementation reduces the risk of these defects, although the biological mechanisms for folate mediated birth defect reduction are unknown (Bean et al., 2011). Epidemiological studies showed that FA supplementation prevented cardiac defects (Bailey and Berry, 2005; Ionescu-Ittu et al., 2009). A recent study demonstrated that human and zebrafish utilize similar one-carbon pathways, and folate metabolism is essential for early zebrafish development including heart (Lee et al., 2012). Our study demonstrated that cardiac defects in zebrafish caused by chronic ethanol exposure, which affects multiple steps of cardiogenesis, could be prevented by FA supplementation. Although the specific molecular mechanisms remain to be defined, it seems reasonable to speculate that FA protects the embryos from ethanol-induced defects by epigenetic mechanisms. It was reported that alcohol exposure changes the DNA methylation pattern and causes epigenetic changes (Ballard et al., 2012; Garro et al., 1991; Kaminen-Ahola et al., 2010; Liu et al., 2009; Zhou et al., 2011b). FA is required for the production of methyl groups, which are subsequently used to methylate DNA during epigenetic events. FA also has antioxidant properties (Ibrahim et al., 2012; Joshi et al., 2001) and might attenuate the ethanol-induced oxidative stress. The diverse effects of ethanol on zebrafish embryo development and the extensive rescue by FA co-supplementation suggest that a global development regulatory mechanism affects various developmental events.

Cardiac defects caused by ethanol treatment during gastrulation, and their prevention by folate supplement, was reported in mice and chick models (Serrano et al., 2010). Our study demonstrated that myocardium and endocardium defects caused by prolonged ethanol exposure in zebrafish could be attenuated by FA supplementation, strongly supporting the hypothesis that folate supplementation prevents a large spectrum of CHDs in FASD.

CONCLUSIONS

This is the first study showing ethanol effects on distinct cardiogenic events and the effect of exposure timing on the persistence of heart defects at larval stages. Our data showed that ethanol exposure interrupted divergent cardiac morphogenesis events, causing heart defects. Additionally, prevention of these defects by retinoic acid or folic acid co-supplementation indicates that these nutritional compounds could mitigate FASD-like defects. Altogether, this study illustrates the complexity of FASD phenotypes and indicates that a single mechanism alone does not explain the entire spectrum of ethanol-induced cardiac defects. Future studies are needed to analyze ethanol effects on different cardiac progenitor populations, which will help elucidate the mechanistic details of FASD-associated heart defects.

EXPERIMENTAL PROCEDURES

Zebrafish husbandry

Zebrafish (*Danio rerio*; TL and AB strains; *Tg[cmlc2:GFP]* and *Tg[fli1:EGFP]* transgenic lines) were raised and housed under standard laboratory conditions (Westerfield, 2000), in accordance with Indiana University Policy on Animal Care and Use.

Ethanol, retinoic acid, and folic acid treatment

Zebrafish embryos were exposed to two different concentrations of ethanol: 100 mM (0.6% v/v) or 150 mM (0.9% v/v), at various developmental stages. 100 mM was the lowest concentration that consistently produced embryos featuring FASD-like phenotype including short body, small head circumference and small eyes. Actual ethanol concentrations within tissues of treated embryos were not measured. RA (Sigma, all trans retinoic acid) concentration was used as described previously (Marrs et al., 2010). This concentration showed no RA induced defects in zebrafish. Different FA (Sigma, F7876-1G) concentrations (10^{-7} M–10^{-5}M) were tested for their ability to consistently rescue ethanol-induced defects. 50 μM FA was the lowest concentration tested that partially rescued ethanol-induced defects. Concentration higher than 75 μM FA could not be tested because FA precipitated out of embryo medium (EM).

For chronic exposure, embryos were maintained in embryo medium until 2 hpf. At this time, embryos were transferred to one of the following conditions: EM (control); EM containing ethanol (100 mM or 150 mM); EM containing ethanol and 1 nM RA; EM containing ethanol and 75 μM FA; EM containing 1 nM RA; and EM containing 75 μM FA. Petri dishes containing embryos were wrapped with parafilm and maintained at 28.5°C. At 24 hpf, respective solutions were replaced with fresh treatment solutions. Embryos were replaced with EM without additions at 48 hpf and examined at various times.

For short exposures, embryos were treated during examined heart development stages with the above solutions, and examined at various times. Embryos were in EM before or after treatment. When needed, embryos were treated with 1-phenyl 2-thiourea (0.003%) to prevent melanogenesis.

Microscopy

Differential interference contrast images of live embryos were collected using a Zeiss Observer Z1 (20X 0.8 NA objective) equipped with an Orca-AG CCD camera (Hamamatsu Photonics). Brightfield images were digitally acquired with a color Leica DFC290 camera mounted on a Leica MZ12 dissecting stereomicroscope (Leica Microsystems, Inc.). Images were also acquired using a Zeiss Observer Z1 LSM 700 confocal microscope (40X 1.1 NA W or 20X 0.8 NA objectives). 3D renderings and Supplementary Movies were produced from images volumes using Volocity software (PerkinElmer/Invitrogen).

Immunofluorescence and F-actin staining

Whole-mount immunostaining was performed as previously described (Clendenon et al., 2012) using primary antibody against alcam (Zn5; ZIRC) at a dilution of 1:250. Texas red-conjugated anti-mouse secondary antibody was used at a 1:100 dilution (Molecular probes/ Invitrogen). Texas red-conjugated phalloidin (Molecular Probes/Invitrogen) was used at a 1:100 dilution.

Cell counting and cell surface measurement

Alcam stained *Tg[cmlc2:GFP]* embryos were imaged with Zeiss Observer Z1 LSM 700 confocal microscope. Ventricular cardiomyocytes were counted using Volocity software 3D

opacity view. Cells in the extended focus images were outlined and surface area of ventricular cardiomyocytes was measured using Volocity software.

In situ hybridization

Whole-mount in situ hybridization of zebrafish embryos was performed as described (Sarmah et al., 2010). Digoxigenin-labeled riboprobes for *cmlc2, vmhc, bmp4, nkx2.5, gata5* and *fgf8* (generously provided by Drs. Ela W. Knapik and Jau-Nian Chen) were synthesized using DIG RNA Labeling Kit (Roche).

Quantitative PCR Analysis

Total RNA was extracted from the whole embryo (~ 20 embryos) at 6s or 12s stages using the TRIzol reagent (Sigma). One microgram of total RNA was reverse transcribed to cDNA using M-MLV reverse transcriptase (Promega), and cDNA was diluted tenfold with RNase free water. Each PCR reaction was performed with 1–4 μl of cDNA using Power SYBR Green PCR mix (Applied Biosystems) and 0.5 μM of each primer. Primer sets used are: hand2-f: GAGTTTAGTTGGAGGGTTTCCCCACC; hand2-r: GTAGTGCGAATGGTCGAGCCCG; fgf8-f1: ACGGACACATTTGGGAGTCGAGTT; fgf8-r1:TCACATTCTGCAGAGCCGTGTAGT; gata5-f1: TTCTCTTATTCGCACAGTCCGCCA; gata5-r1: AGGGCACTTCCATATTGATCCGCA; nkx2.5-f1: TGGGAGACACGTCCACTTACAACA; nkx2.5-r1:TGCTCGACGGATAGTTGCATGAGT; tbx5a-f1: CAGACAAACAGAATGCAGCCGTCA; tbx5a-r1: ACTTTGAAGCTGGGAAACATCCGC; rsp15-f: CAGAGGTGTGGACCTGGACCAGC; rsp15-r: CGGGCAGGATGACCATGTCTCTC. Three independent experiments in triplicate were performed using *rsp15* as internal control. Thermal cycling was carried out either 7300 Real Time PCR System (Applied Biosystems) or LightCycler 480 (Roche).

Statistical Analysis

Statistical analyses were performed using paired two-tailed Student's *t*-test (GraphPad Software) or Mantel-Haenszel chi-square test (Biostatistics services, IUSM).

Supplementary Material

Refer to Web version on PubMed Central for supplementary material.

Acknowledgments

This work was supported by NIH/NIAAA grant P60 AA007611 (PI Dr. David Crabb) and R21AA015938 to (PI Dr. William Bosron; Co-investigator J.A.M.).

Ela W. Knapik (Vanderbilt University Medical Center) and Lila Solnica-Krezel (Washington University, St. Louis) for providing us *Tg[cmlc2:GFP]* and *Tg[fli1:EGFP]* transgenic lines. Plasmid probes to detect *cmlc2, vmhc, fgf8a, gata5*, and *nkx2.5* were generously provided by Ela W. Knapik and Jau-Nian Chen (UCLA). We thank P. Muralidharan, Sameerah T. Alkhairy, C. Curtis and members of the Marrs laboratory for helpful discussion. This work was supported by NIH/NIAAA grant P60 AA007611 (PI Dr. David Crabb) and R21AA015938 to (PI Dr. William Bosron; Co-investigator J.A.M.).

References

Abel EL. An update on incidence of FAS: FAS is not an equal opportunity birth defect. Neurotoxicology and teratology. 1995; 17:437–443. [PubMed: 7565490]

Abel, EL. Fetal alcohol abuse syndrome. Plenum Press; New York: 1998.

Abel EL, Hannigan JH. Maternal risk factors in fetal alcohol syndrome: provocative and permissive influences. Neurotoxicology and teratology. 1995; 17:445–462. [PubMed: 7565491]

Auman HJ, Coleman H, Riley HE, Olale F, Tsai HJ, Yelon D. Functional modulation of cardiac form through regionally confined cell shape changes. PLoS biology. 2007; 5:e53. [PubMed: 17311471]

Bailey LB, Berry RJ. Folic acid supplementation and the occurrence of congenital heart defects, orofacial clefts, multiple births, and miscarriage. The American journal of clinical nutrition. 2005; 81:1213S–1217S. [PubMed: 15883454]

Ballard MS, Sun M, Ko J. Vitamin A, folate, and choline as a possible preventive intervention to fetal alcohol syndrome. Medical hypotheses. 2012; 78:489–493. [PubMed: 22285196]

Bartman T, Walsh EC, Wen KK, McKane M, Ren J, Alexander J, Rubenstein PA, Stainier DY. Early myocardial function affects endocardial cushion development in zebrafish. PLoS biology. 2004; 2:E129. [PubMed: 15138499]

Bean LJ, Allen EG, Tinker SW, Hollis ND, Locke AE, Druschel C, Hobbs CA, O'Leary L, Romitti PA, Royle MH, Torfs CP, Dooley KJ, Freeman SB, Sherman SL. Lack of maternal folic acid supplementation is associated with heart defects in Down syndrome: a report from the National Down Syndrome Project. Birth defects research Part A, Clinical and molecular teratology. 2011; 91:885–893.

Beis D, Bartman T, Jin SW, Scott IC, D'Amico LA, Ober EA, Verkade H, Frantsve J, Field HA, Wehman A, Baier H, Tallafuss A, Bally-Cuif L, Chen JN, Stainier DY, Jungblut B. Genetic and cellular analyses of zebrafish atrioventricular cushion and valve development. Development. 2005; 132:4193–4204. [PubMed: 16107477]

Bingol N, Schuster C, Fuchs M, Iosub S, Turner G, Stone RK, Gromisch DS. The influence of socioeconomic factors on the occurrence of fetal alcohol syndrome. Advances in alcohol & substance abuse. 1987; 6:105–118. [PubMed: 3425475]

Blader P, Strahle U. Ethanol impairs migration of the prechordal plate in the zebrafish embryo. Developmental biology. 1998; 201:185–201. [PubMed: 9740658]

Bruyere HJ Jr, Stith CE. Strain-dependent effect of ethanol on ventricular septal defect frequency in White Leghorn chick embryos. Teratology. 1993; 48:299–303. [PubMed: 8278929]

Burd L, Deal E, Rios R, Adickes E, Wynne J, Klug MG. Congenital heart defects and fetal alcohol spectrum disorders. Congenital heart disease. 2007; 2:250–255. [PubMed: 18377476]

Cavieres MF, Smith SM. Genetic and developmental modulation of cardiac deficits in prenatal alcohol exposure. Alcoholism, clinical and experimental research. 2000; 24:102–109.

Chernyavskaya Y, Ebert AM, Milligan E, Garrity DM. Voltage-gated calcium channel CACNB2 (beta2.1) protein is required in the heart for control of cell proliferation and heart tube integrity. Developmental dynamics: an official publication of the American Association of Anatomists. 2012; 241:648–662. [PubMed: 22274990]

Clendenon SG, Sarmah S, Shah B, Liu Q, Marrs JA. Zebrafish cadherin-11 participates in retinal differentiation and retinotectal axon projection during visual system development. Developmental dynamics: an official publication of the American Association of Anatomists. 2012; 241:442–454. [PubMed: 22247003]

Daft PA, Johnston MC, Sulik KK. Abnormal heart and great vessel development following acute ethanol exposure in mice. Teratology. 1986; 33:93–104. [PubMed: 3738814]

Dlugos CA, Rabin RA. Structural and functional effects of developmental exposure to ethanol on the zebrafish heart. Alcoholism, clinical and experimental research. 2010; 34:1013–1021.

Duester G. A hypothetical mechanism for fetal alcohol syndrome involving ethanol inhibition of retinoic acid synthesis at the alcohol dehydrogenase step. Alcoholism, clinical and experimental research. 1991; 15:568–572.

Fang TT, Bruyere HJ Jr, Kargas SA, Nishikawa T, Takagi Y, Gilbert EF. Ethyl alcohol-induced cardiovascular malformations in the chick embryo. Teratology. 1987; 35:95–103. [PubMed: 3563941]

Garro AJ, McBeth DL, Lima V, Lieber CS. Ethanol consumption inhibits fetal DNA methylation in mice: implications for the fetal alcohol syndrome. Alcoholism, clinical and experimental research. 1991; 15:395–398.

Hamid A, Kaur J. Long-term alcohol ingestion alters the folate-binding kinetics in intestinal brush border membrane in experimental alcoholism. Alcohol. 2007; 41:441–446. [PubMed: 17936512]

Hochgreb T, Linhares VL, Menezes DC, Sampaio AC, Yan CY, Cardoso WV, Rosenthal N, Xavier-Neto J. A caudorostral wave of RALDH2 conveys anteroposterior information to the cardiac field. Development. 2003; 130:5363–5374. [PubMed: 13129847]

Hutson JR, Stade B, Lehotay DC, Collier CP, Kapur BM. Folic acid transport to the human fetus is decreased in pregnancies with chronic alcohol exposure. PLoS One. 2012; 7(5):e38057. [PubMed: 22666445]

Ibrahim W, Tousson E, El-Masry T, Arafa N, Akela M. The effect of folic acid as an antioxidant on the hypothalamic monoamines in experimentally induced hypothyroid rat. Toxicology and industrial health. 2012; 28:253–261. [PubMed: 21967841]

Ionescu-Ittu R, Marelli AJ, Mackie AS, Pilote L. Prevalence of severe congenital heart disease after folic acid fortification of grain products: time trend analysis in Quebec, Canada. BMJ. 2009; 338:b1673. [PubMed: 19436079]

Johnson CS, Zucker RM, Hunter ES, Sulik KK. Perturbation of retinoic acid (RA)-mediated limb development suggests a role for diminished RA signaling in the teratogenesis of ethanol. Birth Defects Res A Clin Mol Teratol. 2007; 79:631–641. [PubMed: 17676605]

Joshi R, Adhikari S, Patro BS, Chattopadhyay S, Mukherjee T. Free radical scavenging behavior of folic acid: evidence for possible antioxidant activity. Free radical biology & medicine. 2001; 30:1390–1399. [PubMed: 11390184]

Kaminen-Ahola N, Ahola A, Maga M, Mallitt KA, Fahey P, Cox TC, Whitelaw E, Chong S. Maternal ethanol consumption alters the epigenotype and the phenotype of offspring in a mouse model. PLoS genetics. 2010; 6:e1000811. [PubMed: 20084100]

Kashyap B, Frey RA, Stenkamp DL. Ethanol-induced microphthalmia is not mediated by changes in retinoic acid or sonic hedgehog signaling during retinal neurogenesis. Alcohol Clin Exp Res. 2011; 35:1644–1661. [PubMed: 21554333]

Keegan BR, Feldman JL, Begemann G, Ingham PW, Yelon D. Retinoic acid signaling restricts the cardiac progenitor pool. Science. 2005; 307:247–249. [PubMed: 15653502]

Klingenberg CP, Wetherill L, Rogers J, Moore E, Ward R, Autti-Ramo I, Fagerlund A, Jacobson SW, Robinson LK, Hoyme HE, Mattson SN, Li TK, Riley EP, Foroud T. Prenatal alcohol exposure alters the patterns of facial asymmetry. Alcohol. 2010; 44:649–657. [PubMed: 20060678]

Lazic S, Scott IC. Mef2cb regulates late myocardial cell addition from a second heart field-like population of progenitors in zebrafish. Developmental biology. 2011; 354:123–133. [PubMed: 21466801]

Leo MA, Lieber CS. Alcohol, vitamin A, and beta-carotene: adverse interactions, including hepatotoxicity and carcinogenicity. The American journal of clinical nutrition. 1999; 69:1071–1085. [PubMed: 10357725]

Lieber CS. Relationships between nutrition, alcohol use, and liver disease. Alcohol research & health: the journal of the National Institute on Alcohol Abuse and Alcoholism. 2003; 27:220–231. [PubMed: 15535450]

Lin CJ, Lin CY, Chen CH, Zhou B, Chang CP. Partitioning the heart: mechanisms of cardiac septation and valve development. Development. 2012; 139:3277–3299. [PubMed: 22912411]

Liu Y, Balaraman Y, Wang G, Nephew KP, Zhou FC. Alcohol exposure alters DNA methylation profiles in mouse embryos at early neurulation. Epigenetics: official journal of the DNA Methylation Society. 2009; 4:500–511. [PubMed: 20009564]

Marrs JA, Clendenon SG, Ratcliffe DR, Fielding SM, Liu Q, Bosron WF. Zebrafish fetal alcohol syndrome model: effects of ethanol are rescued by retinoic acid supplement. Alcohol. 2010; 44:707–715. [PubMed: 20036484]

Mitchell JJ, Paiva M, Heaton MB. The antioxidants vitamin E and beta-carotene protect against ethanol-induced neurotoxicity in embryonic rat hippocampal cultures. Alcohol. 1999; 17:163–168. [PubMed: 10064385]

Niederreither K, Vermot J, Messaddeq N, Schuhbaur B, Chambon P, Dolle P. Embryonic retinoic acid synthesis is essential for heart morphogenesis in the mouse. Development. 2001; 128:1019–1031. [PubMed: 11245568]

Pullarkat RK. Hypothesis: prenatal ethanol-induced birth defects and retinoic acid. Alcoholism, clinical and experimental research. 1991; 15:565–567.

Riikonen R, Salonen I, Partanen K, Verho S. Brain perfusion SPECT and MRI in foetal alcohol syndrome. Developmental medicine and child neurology. 1999; 41:652–659. [PubMed: 10587040]

Ryckebusch L, Wang Z, Bertrand N, Lin SC, Chi X, Schwartz R, Zaffran S, Niederreither K. Retinoic acid deficiency alters second heart field formation. Proceedings of the National Academy of Sciences of the United States of America. 2008; 105:2913–2918. [PubMed: 18287057]

Sarmah S, Barrallo-Gimeno A, Melville DB, Topczewski J, Solnica-Krezel L, Knapik EW. Sec24D-dependent transport of extracellular matrix proteins is required for zebrafish skeletal morphogenesis. PloS one. 2010; 5:e10367. [PubMed: 20442775]

Serrano M, Han M, Brinez P, Linask KK. Fetal alcohol syndrome: cardiac birth defects in mice and prevention with folate. American journal of obstetrics and gynecology. 2010; 203:75e77–75e15. [PubMed: 20451895]

Sirbu IO, Zhao X, Duester G. Retinoic acid controls heart anteroposterior patterning by down-regulating Isl1 through the Fgf8 pathway. Developmental dynamics: an official publication of the American Association of Anatomists. 2008; 237:1627–1635. [PubMed: 18498088]

Stainier DY. Zebrafish genetics and vertebrate heart formation. Nature reviews Genetics. 2001; 2:39–48.

Staudt, D.; Stainier, D. Annual review of genetics. 2012. Uncovering the Molecular and Cellular Mechanisms of Heart Development Using the Zebrafish.

Strandberg-Larsen K, Skov-Ettrup LS, Gronbaek M, Andersen AM, Olsen J, Tolstrup J. Maternal alcohol drinking pattern during pregnancy and the risk for an offspring with an isolated congenital heart defect and in particular a ventricular septal defect or an atrial septal defect. Birth defects research Part A, Clinical and molecular teratology. 2011; 91:616–622.

Thisse, CTB. High Throughput Expression Analysis of ZF-Models Consortium Clones. ZFIN Direct Data Submission. 2005. (http://zfin.org.)

Twal, WOaZ; MH. Retinoic Acid Reverses Ethanol-induced Cardiovascular Abnormalities in Quail Embryos. Alcoholism: Clinical and Experimantal Research. 1997; 21:1137–1143.

Wagner M, Siddiqui MA. Signal transduction in early heart development (II): ventricular chamber specification, trabeculation, and heart valve formation. Exp Biol Med (Maywood). 2007; 232:866–880. [PubMed: 17609502]

Waxman JS, Keegan BR, Roberts RW, Poss KD, Yelon D. Hoxb5b acts downstream of retinoic acid signaling in the forelimb field to restrict heart field potential in zebrafish. Developmental cell. 2008; 15:923–934. [PubMed: 19081079]

Webster WS, Germain MA, Lipson A, Walsh D. Alcohol and congenital heart defects: an experimental study in mice. Cardiovascular research. 1984; 18:335–338. [PubMed: 6744353]

Westerfield, M. The zebrafish book. Eugene, OR: The University of Oregon Press; 2000.

Xavier-Neto J, Rosenthal N, Silva FA, Matos TG, Hochgreb T, Linhares VL. Retinoid signaling and cardiac anteroposterior segmentation. Genesis. 2001; 31:97–104. [PubMed: 11747199]

Yelin R, Schyr RB, Kot H, Zins S, Frumkin A, Pillemer G, Fainsod A. Ethanol exposure affects gene expression in the embryonic organizer and reduces retinoic acid levels. Developmental biology. 2005; 279:193–204. [PubMed: 15708568]

Zachman RD, Grummer MA. The interaction of ethanol and vitamin A as a potential mechanism for the pathogenesis of Fetal Alcohol syndrome. Alcoholism, clinical and experimental research. 1998; 22:1544–1556.

Zhang Y, Shao M, Wang L, Liu Z, Gao M, Liu C, Zhang H. Ethanol exposure affects cell movement during gastrulation and induces split axes in zebrafish embryos. Int J Dev Neurosci. 2010; 28(4): 283–288. [PubMed: 20394815]

Zhou FC, Balaraman Y, Teng M, Liu Y, Singh RP, Nephew KP. Alcohol alters DNA methylation patterns and inhibits neural stem cell differentiation. Alcoholism, clinical and experimental research. 2011a; 35:735–746.

Zhou Y, Cashman TJ, Nevis KR, Obregon P, Carney SA, Liu Y, Gu A, Mosimann C, Sondalle S, Peterson RE, Heideman W, Burns CE, Burns CG. Latent TGF-beta binding protein 3 identifies a second heart field in zebrafish. Nature. 2011b; 474:645–648. [PubMed: 21623370]

- Zebrafish FASD model showed that ethanol interrupts multiple steps of cardiogenesis.
- Ethanol exposure during zebrafish cardiogenesis produces persistent heart defect.
- Chronic ethanol exposure during cardiogenesis produces complex cardiac defects.
- Retinoic acid co-supplementation partially rescues ethanol induced cardiac defect.
- Folic acid co-supplementation prevents wide spectrum of ethanol-induced heart defects.

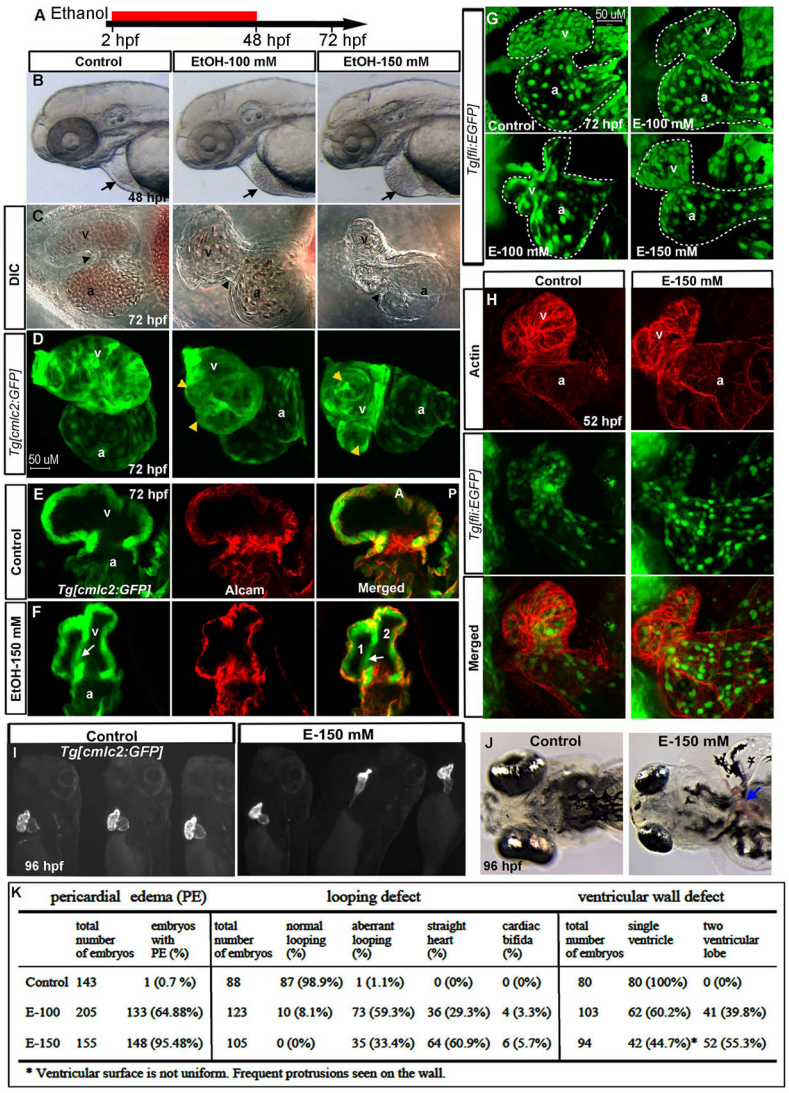

K

	pericardial edema (PE)		looping defect					ventricular wall defect		
	total number of embryos	embryos with PE (%)	total number of embryos	normal looping (%)	aberrant looping (%)	straight heart (%)	cardiac bifida (%)	total number of embryos	single ventricle	two ventricular lobe
Control	143	1 (0.7 %)	88	87 (98.9%)	1 (1.1%)	0 (0%)	0 (0%)	80	80 (100%)	0 (0%)
E-100	205	133 (64.88%)	123	10 (8.1%)	73 (59.3%)	36 (29.3%)	4 (3.3%)	103	62 (60.2%)	41 (39.8%)
E-150	155	148 (95.48%)	105	0 (0%)	35 (33.4%)	64 (60.9%)	6 (5.7%)	94	42 (44.7%)*	52 (55.3%)

* Ventricular surface is not uniform. Frequent protrusions seen on the wall.

Figure 1. Chronic ethanol exposure during cardiogenesis severely disrupts heart formation

(A) Schematic diagram showing the developmental timing (2–48 hpf) of ethanol exposure. (B, C) Live images showed pericardial edema (arrows) (B), and smaller, misshapen chambers with aberrant AV canal (arrowheads) in the ethanol treated embryos (C). (D, G) 3D renderings of confocal sections of *Tg[cmlc2:GFP]* and *Tg[fli1:EGFP]* embryos showing distorted myocardium, multilobed ventricle (D), and misshapen endocardium (G) in ethanol exposed embryos. Yellow arrowheads: multiple lobes. (E, F) Single confocal sections at the AV boundary of alcam-stained *Tg[cmlc2:GFP]* embryos showing a single ventricle in the control and two ventricular lobes (1 & 2) in the ethanol treated embryo. White arrows: abnormal additional ventricular wall connection. (H) Confocal images of Texas red-phalloidin stained *Tg[fli1:EGFP]* embryos showing defective endocardium corresponding to the myocardium in ethanol exposed embryos. (I, J) Brightfield live images of *Tg[cmlc2:GFP]* embryos showed abnormal heart (I) and blood clot (J; blue arrow) at 96 hpf in ethanol exposed embryos. (K) Scores showing the effect of ethanol on cardiac development (Results from three individual experiments). Mantel-Haenszel chi-square

tests:PE, P<0.0001; looping defect, P<0.0001; ventricular wall defect, P<0.0001. a, atrium; v, ventricle. Anterior to the left (B–H, J), anterior to the top (I).

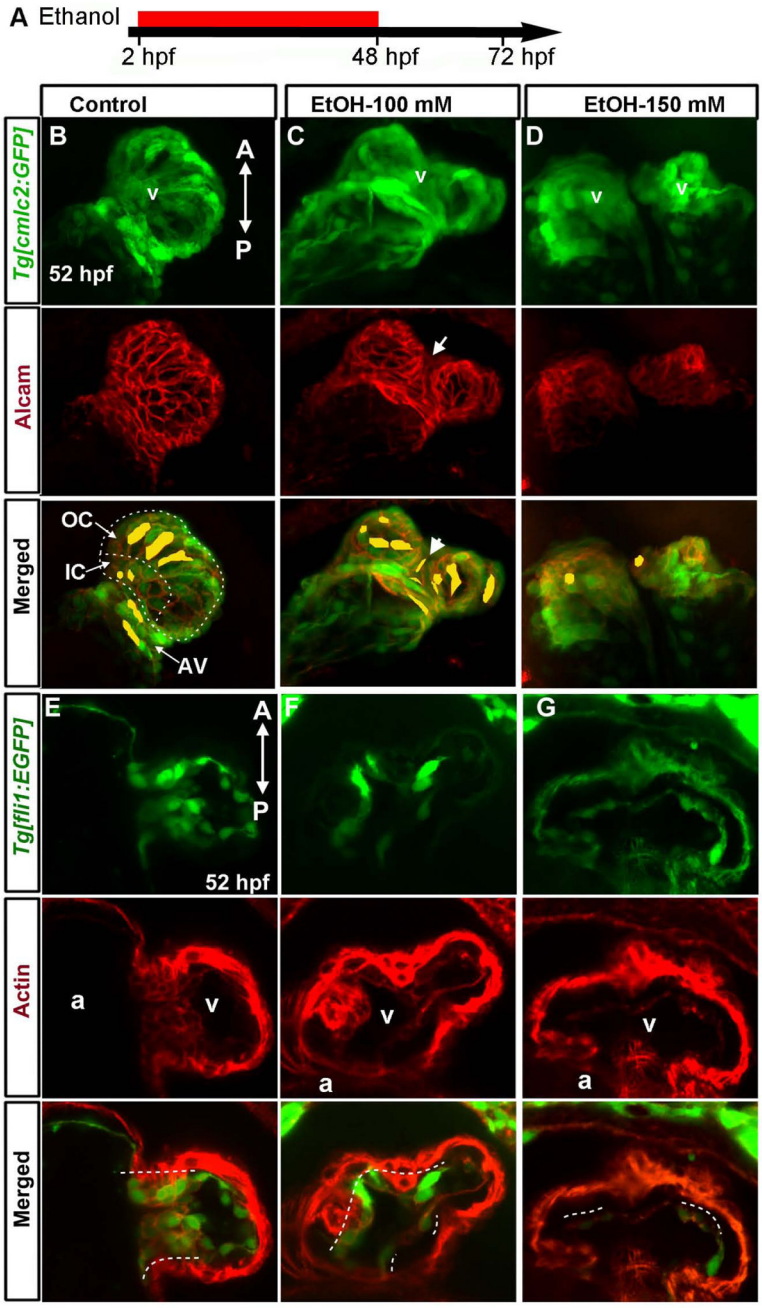

Figure 2. Chronic ethanol exposure during cardiogenesis produces defective chambers and endocardial cushion

(A) Schematic diagram showing the developmental timing (2–48 hpf) of ethanol exposure. (B–D) Ethanol treated embryos do not have stereotypical regionally confined cardiomyocyte shapes. Extended focus images of confocal sections from control *Tg[cmlc2:GFP]* embryo (B) costained with alcam antibody showed large, elongated cardiomyocytes in the outer curvature (OC) and AV region, and small rounded cardiomyocyte in the inner curvature (IC) of the ventriclular surface in control embryos; the orientation of the cells were aligned with each other. (C) Cardiomyocytes were disorganized, showing variable sizes and shapes in

ethanol treated embryos. (D) Ethanol treatment occasionally caused cardia bifida, which display small cardiomyocytes. Representative cell shapes are highlighted in yellow; white arrowhead: abnormal thin cell. (E–G) Severely defective endocardial cushion formation was seen after ethanol treatment. (E) Confocal sections of the control 52 hpf *Tg[fli1:EGFP]* embryo heart co-labeled with Texas red-phalloidin (F-actin), showed clusters of GFP and F-actin positive cells (white dotted line) at the AV boundary, which were reduced (F) or absent (G) in ethanol treated embryos. A: anterior, P: posterior, a: atrium, v: ventricle.

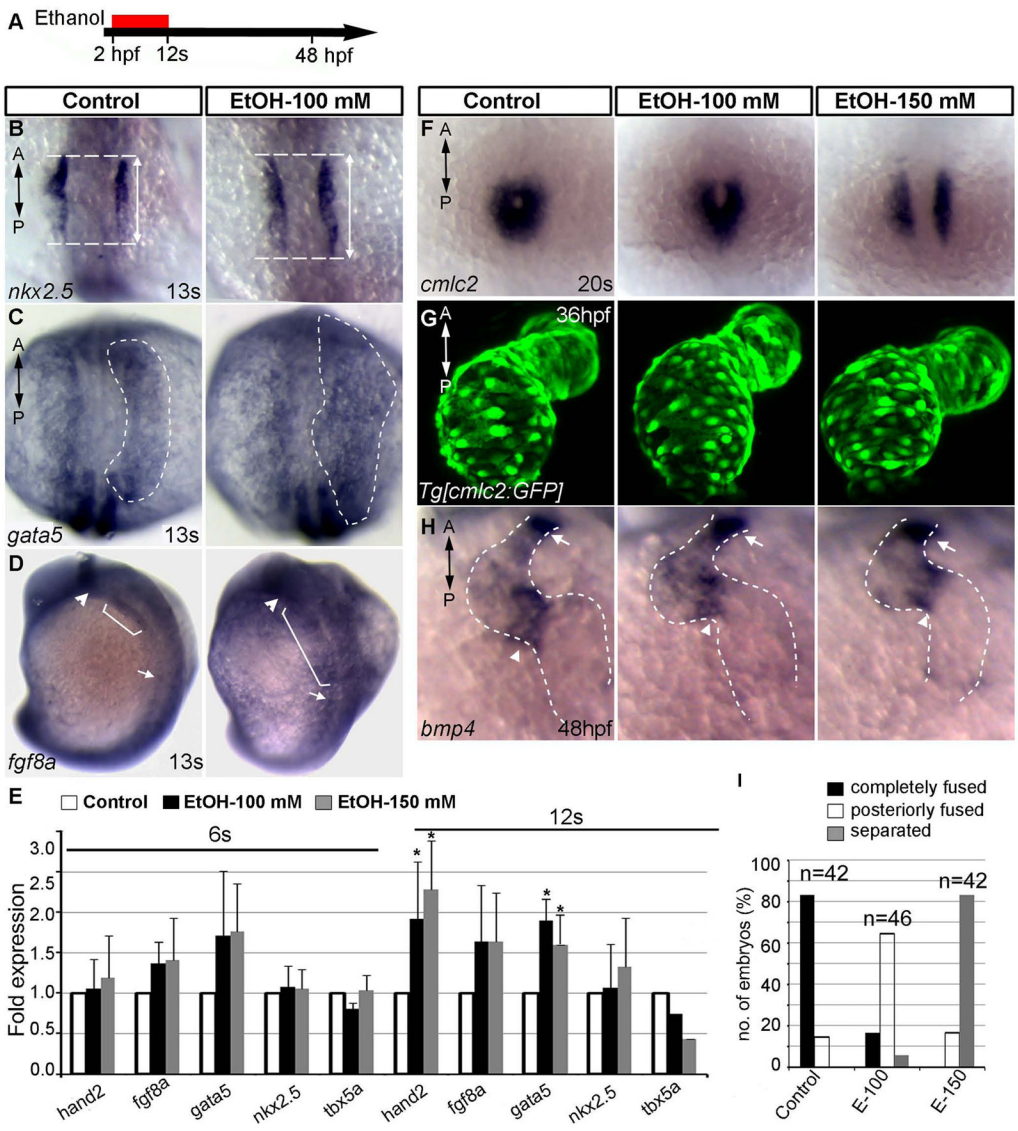

Figure 3. Ethanol exposure during gastrulation through cardiac specification induces defects in cardiac gene expression and myocardial migration

(A) Schematic diagram shows the timing of ethanol exposure. (B–D) Whole mount *ISH* at 13s stages showed moderate expansion of expression domains for *nkx2.5* (B) (see figure 7C for statistical significance), *gata5* (C), and *fgf8a* (D) in the ethanol treated embryos, as compared to control. (E) Transcript levels of genes expressed in differentiating myocardial cells increased after ethanol treatment. Quantitative RT-PCR assays comparing cardiogenic gene expression levels at 6s and 12s stages (average fold change from at least 3 independent experiments), Student's *t*-test: *P<0.01. (F) ISH detecting *cmlc2* at 20s stage showed cardiac fusion delay after ethanol treatment (2 hpf–12s). (G) Live images of *Tg[cmlc2:GFP]* embryos exposed to ethanol (2 hpf–12s) showed normal cardiac looping and normal chamber morphology. (H) *bmp4* expression examined by ISH. Ethanol exposed (2 hpf–12s) embryos showed normal *bmp4* expression pattern. Arrowheads: AV boundary; arrows: OFT; dotted line: cardiac silhouette. (I) Graph illustrates myocardial fusion differences at 20s

stage in control and ethanol treated embryos. Mantel-Haenszel chi-square tests: $P<0.0001$ for both control vs. EtOH-100 and control vs. EtOH-150. n: number of embryos. A: anterior, P: posterior.

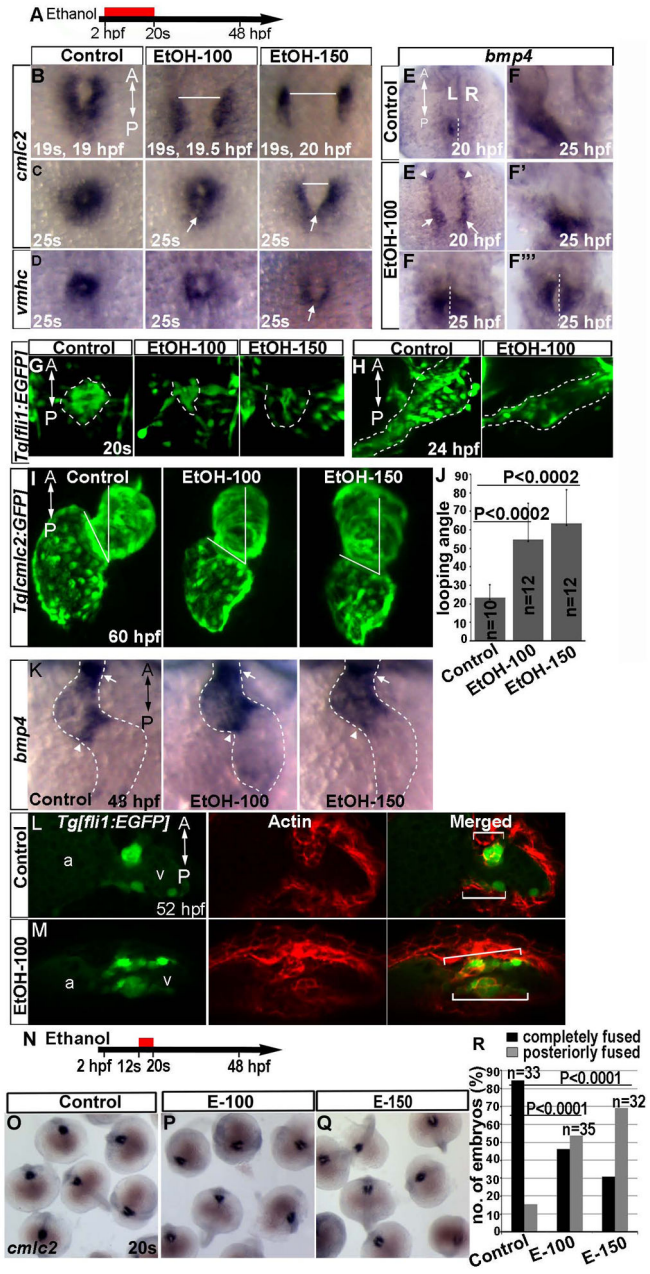

Figure 4. Ethanol exposure until cardiac fusion produces defects that persist at later stages of development

(A, N) Schematic diagrams showing the timing of ethanol exposure. (B–D) ISH of *cmlc2* expression at 19s and 25s; *vmhc* expression at 25s showed delay in myocardial fusion in ethanol exposed embryos. Arrows: posterior fusion. (E, E′) *bmp4* expression at 20 hpf. (E) Control, (E′) ethanol exposed embryos. Arrow: cardiac primordium; arrowhead: posterior retina. (F–F‴) *bmp4* expression at 25hpf. (F) Control, (F′–F‴) representatives of ethanol exposed embryos. (G, H) *Tg[fli1:EGFP]* embryo images at 20s (G) and 24 hpf (H) stages showed defective endocardium formation after ethanol exposure. (I) *Tg[cmlc2:GFP]* embryo images showed aberrant looping angle. (J) Graph shows quantification of looping

angle. (K) *bmp4* expression in the control and ethanol exposed embryos at 48 hpf. Arrowhead: AV boundary; arrow: OFT. (L, M) Stained *Tg[fli1:EGFP]* embryos showed dispersion of GFP and F-actin positive cells (white brackets) throughout the ventricle after ethanol exposure. (N–R) Ethanol exposure only during myocardial migration (12s–20s) causes modest fusion delay. (O–Q) ISH showed *cmlc2* expression. (O) Control, (P,Q) ethanol exposed embryos. (R) Graph shows quantification of myocardial precursors fusion. (P-value: Mantel-Haenszel chi-square tests). A: anterior, P: posterior.

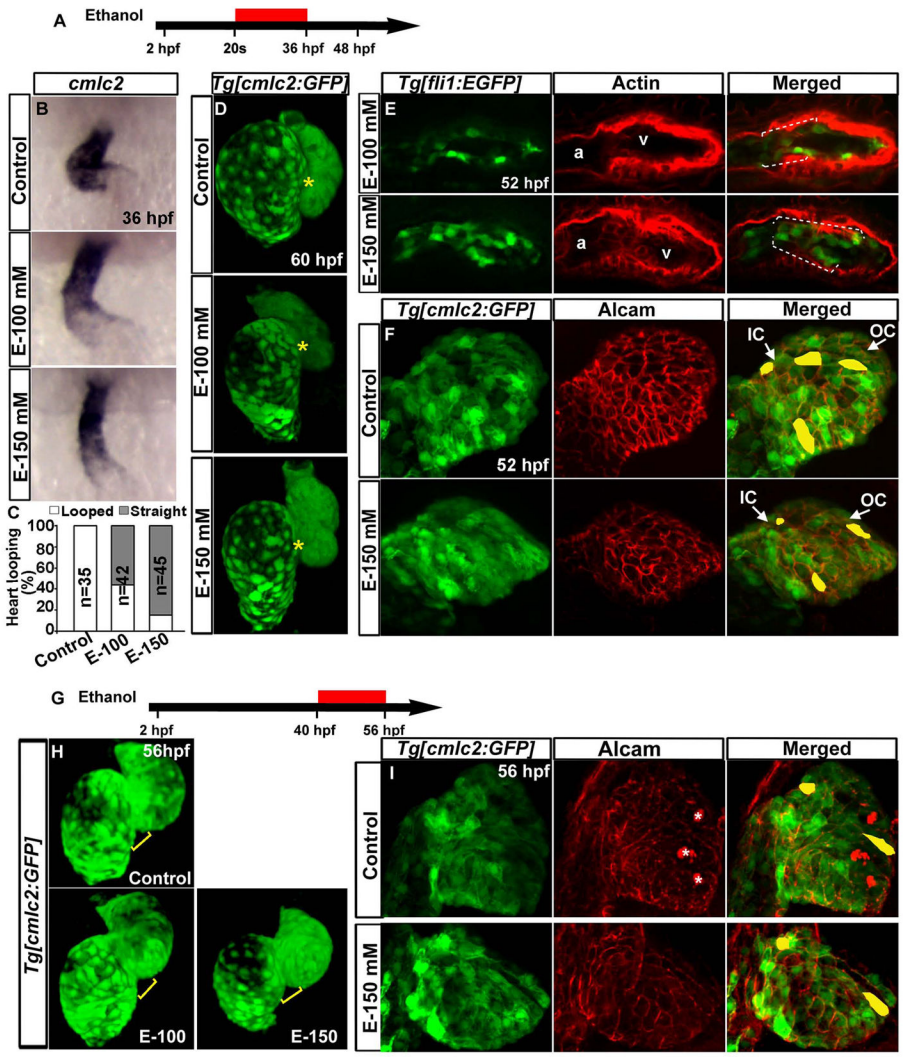

Figure 5. Ethanol exposure during cardiac looping caused abnormal heart morphogenesis and defective endocardial cushions

(A, G) Schematic diagram showing ethanol exposure timing. (B) ISH detecting *cmlc2* at 36 hpf: control, normal looping; EtOH-100 mM, modest looping; EtOH-150 mM, straight heart tube. (C) Graph quantifies looped and straight heart at 36 hpf. (D) 3D confocal images of *Tg[cmlc2:GFP]* embryos: control, normal heart chambers; ethanol treated embryos, aberrant heart chambers. Yellow asterisks: AV canal. (E) Ethanol treated *Tg[fli1:EGFP]* embryos showed dispersed GFP and F-actin positive cells (white dashed line) throughout the ventricle (compare control panel 2E). (F) Alcam stained *Tg[cmlc2:GFP]* embryo showed similar distribution of cardiomyocytes in the control and ethanol treated embryos. (G–I) Ethanol exposure during cardiac chamber morphogenesis did not lead to defective chamber wall formation. (H) 3D confocal images of *Tg[cmlc2:GFP]* embryos: control and E-100 mM, normal heart; E-150, nearly normal heart chamber. Yellow brackets: AV region. (I) Alcam stained *Tg[cmlc2:GFP]* embryos showed similar pattern of cardiomyocyte distribution in the ventricular wall in ethanol treated and control embryos. White asterisk:

alcam positive hatching gland cells, which are outside the heart but seen in this 3D rendering. Representative cell shapes are highlighted in yellow. Anterior to the top.

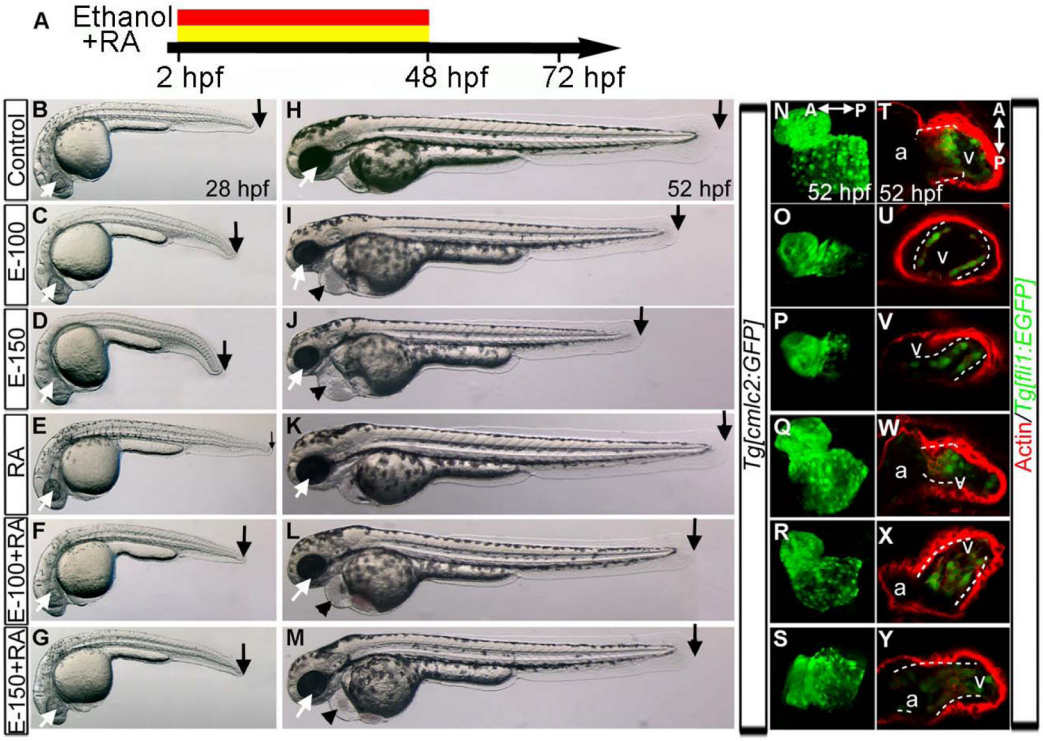

Figure 6. RA Supplementation during chronic ethanol treatment (2–48hpf) does not restore normal heart development

(A) Schematic diagram showing the timing of ethanol and RA exposure. (B–M) Live images of embryos at 28 (B–G) and 52 hpf (H–M) showed normal morphology in the control (B, H) and RA treated (E, K) embryos. Ethanol treated embryos exhibited small eye, shorter body (C, D, I, J) and pericardial edema (I, J). Ethanol+RA treated embryos showed near normal eye size, slightly shorter body (F, G, L, M) and pericardial edema (L, M). Arrows: black, posterior end of the embryos; white: eye; arrowhead: pericardial edema. (N–S) 3D renderings of fixed *Tg[cmlc2:GFP]* embryo confocal sections showed normal cardiac morphology in control (N) and RA treated embryos (Q); straight hearts in ethanol treated embryos (O, P); near normal or straight heart in ethanol+RA cotreated (R, S) embryos. (T, Y) Phalloidin stained *Tg[fli1:EGFP]* embryos: clustering of GFP/F-actin positive cells (white dashed line) at the AV boundary in the control (T) and RA treated embryos (W); reduction and dispersion of GFP/F-actin positive cells in ethanol treated embryos (U, V); dispersion of GFP/F-actin positive cells throughout the ventricle in ethanol+RA cotreated embryos (X, Y). A, anterior; P, posterior.

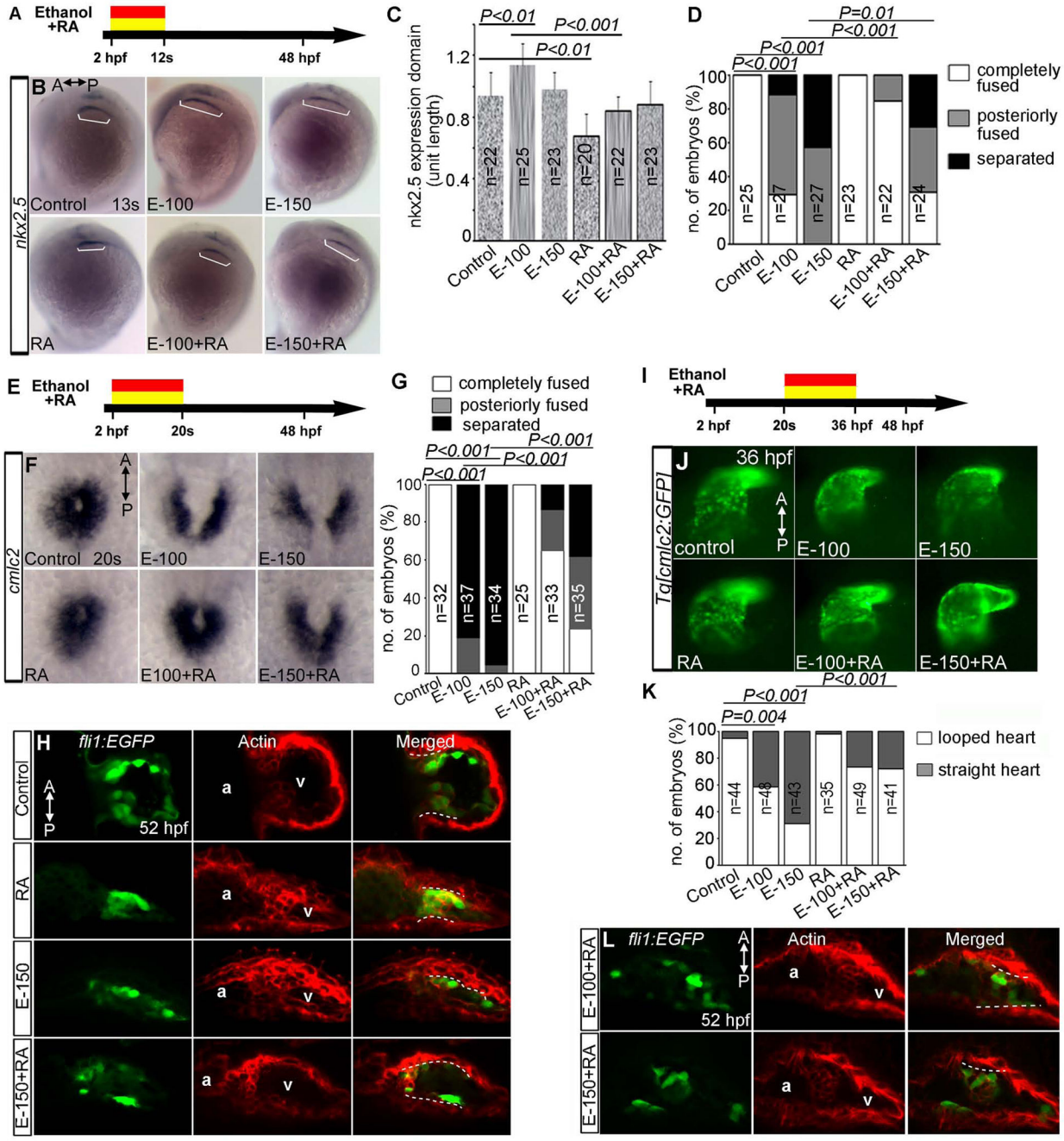

Figure 7. RA supplementation during acute ethanol treatment partially rescues a subset of cardiac development defect

(A, E, I) Schematic diagrams showing the timing of ethanol and RA exposure. (B) ISH showed *nkx2.5* expression in the control, ethanol, RA, and ethanol+RA treated embryos (2hpf–12s). (C) Graph shows the quantification of *nkx2.5* expressing domain length after ethanol exposure (2hpf–12s). (D) Graph shows quantification of myocardial fusion at 20s after ethanol exposure (2hpf–12s). (F) Expression of *cmlc2* in the control, ethanol, RA, and ethanol+RA treated embryos (2hpf–20s). (G) Graph shows the quantification of myocardial fusion. (H) Stained *Tg[fli1:EGFP]* embryos showed the dispersion of GFP and F-actin

positive cells (white dashed line) throughout the ventricle in the ethanol and ethanol+RA cotreated embryos (2hpf–20s). (J) Brightfield images of *Tg[cmlc2:GFP]* embryos showed hearts of control, ethanol, RA, and ethanol+RA treated (20s–36hpf) embryos. (K) Graph showing the quantification of looped and straight heart (as in E-150) at 36 hpf (L) Stained *Tg[fli1:EGFP]* embryos showed reduced clustering of GFP, F-actin double positive cells near the AV boundary in ethanol+RA treated (20s–36 hpf) embryos (Compare control panel 7H; ethanol 5E). Statistical analyses: C, Student's *t*-tests; D, G, K, Mantel-Haenszel chi-square tests.

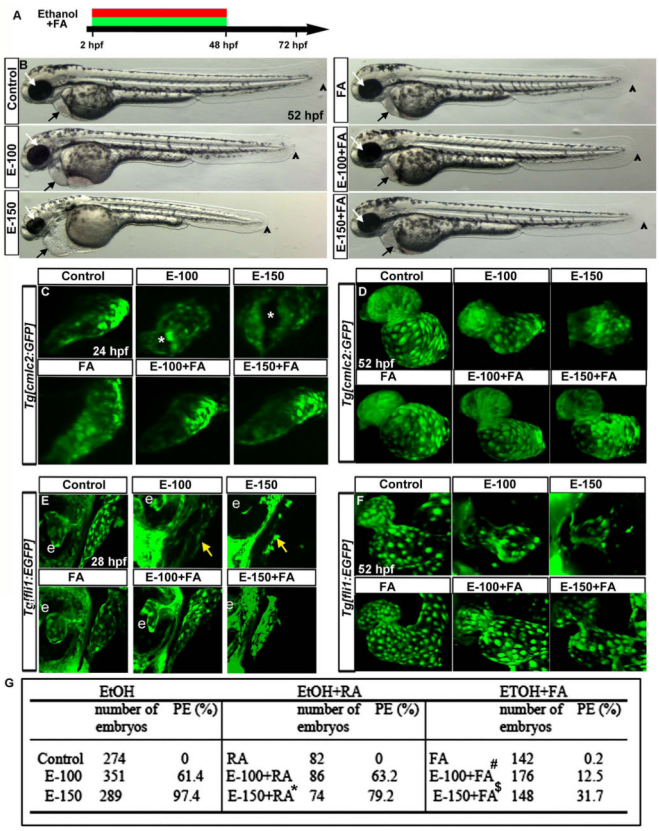

G

EtOH			EtOH+RA			ETOH+FA		
	number of embryos	PE (%)		number of embryos	PE (%)		number of embryos	PE (%)
Control	274	0	RA	82	0	FA	142	0.2
E-100	351	61.4	E-100+RA	86	63.2	E-100+FA#	176	12.5
E-150	289	97.4	E-150+RA*	74	79.2	E-150+FA$	148	31.7

Figure 8. FA supplementation during chronic ethanol exposure (2–48hpf) rescues ethanol-induced cardiac defects

(A) Schematic diagram showing the timing of ethanol and FA exposure. (B) Live images showed heart edema, small eye, and short body length in the ethanol exposed embryos and normal morphology in FA cosupplemented (2–48hpf) embryos. Arrow: black, heart; white: eye; arrowhead: posterior end of the embryo. (C, D) Confocal images of *Tg[cmlc2:GFP]* embryos showed linear heart tube (24 hpf) and normal chambers (52 hpf) in the control, FA treated, and ethanol+FA cotreated embryos. Ethanol exposed embryos exhibited abnormal heart tube with defective myocardial fusion (asterisk, 24 hpf) and misshapen hearts (52 hpf). (E, F) Confocal images of *Tg[fli1:EGFP]* at 28 and 52 hpf showed misshapen endocardium (yellow arrows; e, eye) in the ethanol treated; normal endocardium in control, FA treated, and E-100+FA cotreated; and near normal endocardium in E-150+FA cotreated embryos. (G) Scores showing the effect of continuous supplement of RA or FA with ethanol on pericardial edema (PE). Results shown were calculated from three individual experiments. (Mantel-Haenszel chi-square tests: control vs. EtOH-100 or EtOH-150, P<0.0001; control vs. RA, P=1.00; EtOH-150 vs. EtOH-150+RA, P<0.0001 (*); control vs. FA, P=0.01;EtOH-100 vs. EtOH-100+FA, P<0.0001 (#); EtOH-150 vs. EtOH-150+FA, P<0.0001 ($)).

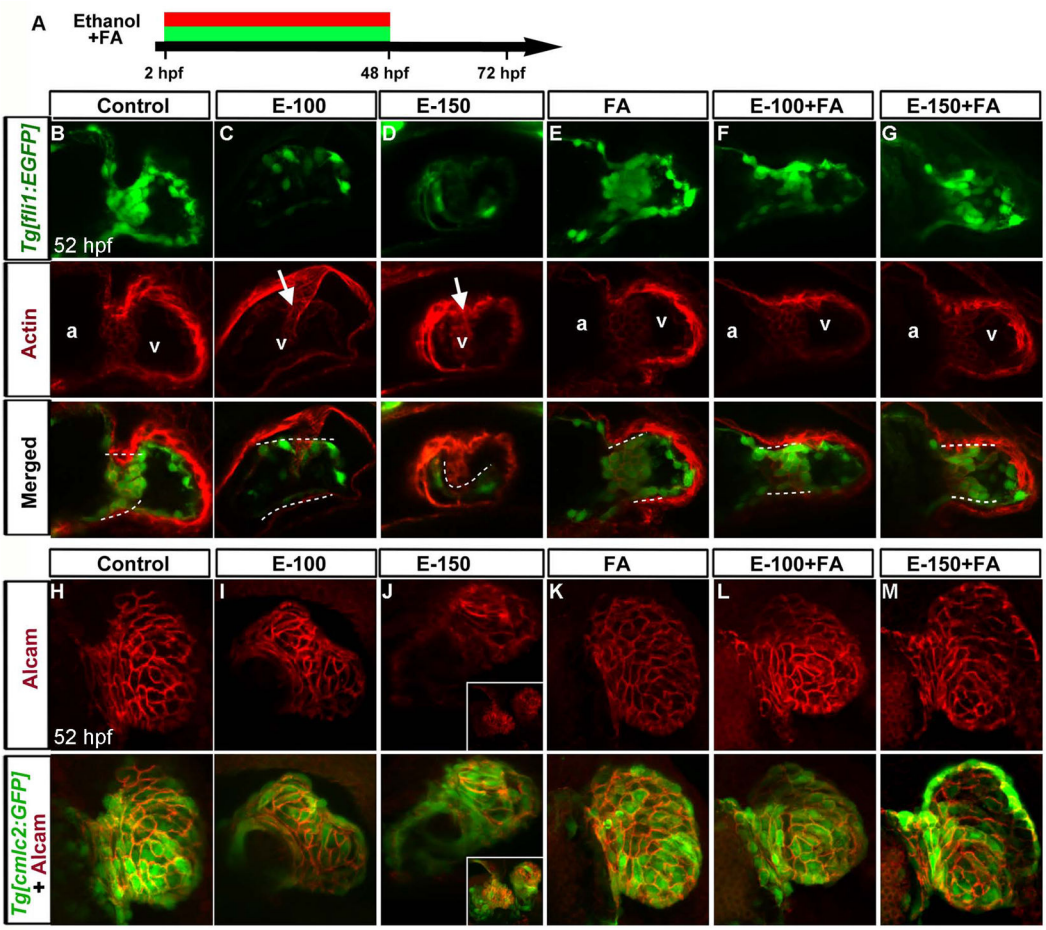

Figure 9. Folic acid supplementation during chronic ethanol exposure (2–48 hpf) rescues ethanol-induced endocardial cushion and chamber formation defects

(A) Schematic diagram showing the timing of ethanol and FA exposure. (B–G) Endocardial cushion formation was restored in ethanol exposed, FA co-supplemented embryos. Stained *Tg[fli1:EGFP]* embryos showed clustering of GFP and F-actin positive cells (white dashed line) in the control, FA treated, and ethanol+FA co-treated embryos. Ethanol treated embryos exhibited no clustering of GFP and F-actin positive cells at the AV boundary. White arrow: defective wall in the ventricle. a, atrium; v, ventricle. Atrium in the ethanol treated embryos cannot be seen in this view. (H–M) Ethanol-induced ventricular chamber defects were rescued in the FA cosupplemented embryos. Alcam stained *Tg[cmlc2:GFP]* embryos showed similar pattern of cardiomyocyte distribution in the ventricular wall of control, FA treated, and ethanol+FA cotreated embryos; cardiomyocyte sizes and shapes were variable throughout the ventricular wall in the ethanol treated embryos. Inset in 150 mM ethanol showed cardia bifida. Anterior to the top.